

Dear Editor,

Thank you for your positive decision. After the constructive, and positive, remarks of the editors, we replied to their concerns in detail and clarified the points on which misunderstanding was raised in the discussion forum. We have made some corrections in the formulations and made some textual corrections. Also we clarified the descriptions of the figures. Finally, we added a table with notations of the parameters used. The marked-up version shows all the changes made to the original draft.

Thank you again for the review process. We hope that the final version is found in order.

Sincerely,  
Hubert Savenije  
Zhilin Zhang

# Thermodynamics of Saline and Fresh Water Mixing in Estuaries

Zhilin Zhang and Hubert H.G. Savenije

[Department of Water Management](#), Delft University of Technology, [Delft, the Netherlands](#)

## Abstract

Mixing of saline and fresh water is a process of energy dissipation. The fresh water flow that enters an estuary from the river contains potential energy with respect to the saline ocean water. This potential energy is able to perform work. Looking from the ocean to the river, there is a gradual transition from saline to fresh water and an associated rise of the water level in accordance with the increase of potential energy. Alluvial estuaries are systems that are free to adjust dissipation processes to the energy sources that drive them, primarily the kinetic energy of the tide and the potential energy of the river flow, and to a minor extent the energy in wind and waves. Mixing is the process that dissipates the potential energy of the fresh water. The Maximum Power (MP) concept assumes that this dissipation takes place at maximum power, whereby the different mixing mechanisms of the estuary jointly perform the work. In this paper, the power is maximized with respect to the dispersion coefficient that reflects the combined mixing processes. The resulting equation is an additional differential equation that can be solved in combination with the advection-dispersion equation, requiring only two boundary conditions for the salinity and the dispersion. The new equation has been confronted with 52 salinity distributions observed in 23 estuaries in different parts of the world and performs very well.

## 1. Introduction

Mixing of fresh and saline water in estuaries is governed by the dispersion-advection equation, which results from the combination of the salt balance and the water balance under partial to well-mixed conditions (see e.g., Savenije, 2005). The partially to well-mixed condition applies when the increase of the salinity over the [estuarine](#) depth is gradual. The salinity equation reads:

$$A_s \frac{\partial S}{\partial t} + Q \frac{\partial S}{\partial x} - \frac{\partial}{\partial x} \left( AD \frac{\partial S}{\partial x} \right) = 0 \quad (1)$$

Here,  $S$  [psu] is the salinity of the water,  $Q$  [ $L^3T^{-1}$ ] is the water flow in the estuary,  $A$  [ $L^2$ ] is the cross-sectional area of the flow (not necessarily equal to the storage cross section  $A_s$ ),  $x$  is the [distance from the estuary mouth](#), and  $D$  [ $L^2T^{-1}$ ] is the dispersion coefficient. The first term reflects the change of the salinity over time as a result of the balance between the advection by the water flow (second term) and the mixing of water with different salinity by dispersive exchange flows (third term). If there is no other source of salinity, then the sum of these terms is zero. If we average this equation over a tidal period, then the first term reflects the long term change of the salinity as a result of the balance between the advection of fresh water from the river and the tidal average exchange flows. In a steady state, where the first term is zero, the equation can be simply integrated with respect to  $x$ , yielding:

$$Q(S - S_f) - AD \frac{dS}{dx} = 0 \quad (2)$$

with the condition that at the upstream boundary  $dS/dx = 0$  and  $S = S_f$ , the salinity of the fresh river water. In the steady state situation the discharge  $Q$  then equals the freshwater discharge coming from upstream, which has a negative value moving seaward; similarly the salinity gradient  $S' = dS/dx$  is negative with the salinity decreasing in upstream direction. Assuming that in a given estuary the geometry  $A(x)$  is known, as well as the observed salinity and discharge of the fresh river water, then this differential equation has two unknowns  $D(x)$  and  $S(x)$ .

hsavenije 5/1/2018 08:38

Deleted: e

hsavenije 5/1/2018 08:37

Deleted: d

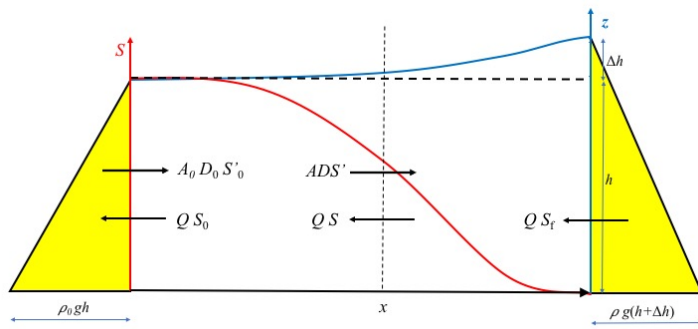
Unknown

Field Code Changed

50  
51  
52  
53  
54  
55  
56  
57  
58  
59  
60  
61

In the steady state, the flushing out of salt by the fresh river discharge is balanced by the exchange of saline and fresh water resulting from a combination of mixing processes, which causes an upriver flux of salt. The sketch in Figure 1 presents the system description with a typical longitudinal salinity distribution (in red). It also shows the associated water level (in blue), which has an upstream gradient due to the decreasing salinity. Because of the density difference, the hydrostatic pressures on both sides (in yellow) are not equal. The water level at the toe of the salt intrusion curve is  $\Delta h$  higher, resulting in a seaward pressure difference near the surface and an inland pressure difference near the bottom. Although the hydrostatic forces (the integrals of the hydrostatic pressure distributions) are equal and opposed in steady state, they have different working lines, a distance  $\Delta h/3$  apart. This triggers an angular momentum, which drives the gravitational circulation.

hsavenije 5/1/2018 08:44  
Deleted: that



62  
63  
64  
65  
66

Figure 1. System description of the salt and fresh water mixing in an estuary, with the seaside on the left and the riverside on the right. The water level (blue line) has a slope as a result of the salinity distribution (red line). In yellow are the hydrostatic pressure distributions on both sides. The black arrows show the fluxes. Subscript '0' represents the downstream boundary condition.

67  
68  
69  
70  
71  
72  
73  
74  
75

The dispersion coefficient of Eq. (2) is generally determined by calibration on observations of  $S(x)$ , or predicted by (semi-)empirical methods. Providing a theoretical basis for the dispersion coefficient is not trivial. A fundamental question is what this dispersion actually is. Is it a physical parameter, or merely a parameter that follows from averaging the complex turbulent flow patterns in a natural watercourse? MacCready (2004), for instance, was able to derive an analytical expression for the dispersion as a function of the salinity gradient in addition to geometric, hydraulic, and turbulence parameters. But also this derivation required simplifying assumptions.

76  
77  
78  
79  
80  
81  
82

The complication is that there are many different mixing processes at work. One can distinguish: tidal shear, tidal pumping, tidal trapping, gravitation circulation (e.g., Fischer et al., 1979) and residual circulation due to the interaction between ebb and flood channels (Nguyen and Savenije, 2008; Zhang and Savenije, 2017). And these different processes can be split up in many subcomponents. Park and James (1990), for instance, distinguished 66 components, grouped into 11 terms. This reductionist approach, unfortunately, did not lead to more insight.

83  
84  
85  
86

## 2. Applying thermodynamics to salt and freshwater mixing

Here we take a system's approach, where the assumption is that the different mechanisms are not independent but are jointly at work to reduce the salinity gradient that drives the exchange flows. We use the concept of Maximum Power, as described by Kleidon (2016). Kleidon defines Earth

88 system processes as dissipative systems that do conserve mass and energy, but export entropy.  
 89 These systems tend to function at maximum power, whereby the power of the system can be  
 90 defined as the product of a process flux and the gradient driving the flux. The ability to maintain  
 91 this power (i.e., work through time) in steady state results from the exchange fluxes at the system  
 92 boundary, and when work is performed at the maximum possible rate within the system  
 93 (“Maximum Power”), this equilibrium state reflects the conditions at the system boundary. The key  
 94 parameter describing the process can then be found by maximizing the power.

96 From an energy perspective, we see that the freshwater flux, which has a lower density than saline  
 97 water and, without a counteracting process would float on top of the saline water, adds potential  
 98 energy to the system, while the tide, which flows in and out of the estuary at a regular pace, creates  
 99 turbulence, mixes the fresh and saline water and hence works at reducing this potential energy. This  
 100 is why dispersion predictors are generally linked to the estuarine Richardson number, which  
 101 represents the ratio of the potential energy of the fresh water entering the estuary to the kinetic  
 102 energy of the tidal flow.

104 In thermodynamic terms, the freshwater flux maintains a potential energy gradient, which triggers  
 105 mixing processes that work at depleting this gradient. Because the strength of the mixing of fresh  
 106 and saline water in turn depends on this gradient, there is an optimum where the mixing process  
 107 performs at maximum power. From a system point of view, it is not really relevant which particular  
 108 mixing process is dominant, or how these different processes jointly reduce the salinity gradient.  
 109 What is relevant is how the optimum flux associated with this mixing process, yielding maximum  
 110 power, depends on the dispersion.

112 In our case, the power derived from the potential energy of the freshwater flux is described by the  
 113 product of the upstream dispersive water flux and the gradient in geopotential height driving this  
 114 flux, or alternatively, the product of the dispersive exchange flux and the water level gradient. The  
 115 optimum situation is achieved when the system is in equilibrium state.

117 The water level gradient follows from the balance between the hydrostatic pressures of fresh and  
 118 saline water (see e.g., Savenije, 2005), resulting in:

$$119 \frac{\partial z}{\partial x} = -\frac{h}{2\rho} \frac{\partial \rho}{\partial x} \quad (3)$$

120 where  $z (=h+\Delta h)$  [L] is the tidal average water level (blue line in Figure 1),  $h$  [L] is the tidal  
 121 average water depth (horizontal dash line in Figure 1) and  $\rho$  [ML<sup>-3</sup>] is the depth average density of  
 122 the saline water. The depth gradient is essential for the density driven mixing, but  $\Delta h$  is small  
 123 compared to  $h$  (typically 1.2 % of  $h$ ). Note that this equation applies to the case where the river flow  
 124 velocity is small, which is the case when estuaries are well mixed. Otherwise a backwater effect  
 125 should be included, but this only applies to a situation of high river discharge when the salt intrudes  
 126 by means of a salt wedge with a sharp interface.

127  
 128 One can express the density of saline water as a function of the salinity:  $\rho = 1000 + \alpha_1 S$  where  $\alpha_1$   
 129 is a constant with a value of about 25/35, because seawater with a salinity of 35 psu has a density of  
 130 about 1025 kg/m<sup>3</sup>. As a result, eq. (3) can be written as:

$$131 \frac{\partial z}{\partial x} = -\alpha_1 \frac{h}{2\rho} S' \quad (4)$$

132 The upstream dispersive flux is implicit in the salt balance equation (2), which in steady state can  
 133 be written as:

$$134 Q(S - S_f) = ADS' \quad (5)$$

hsavenije 5/1/2018 08:57  
 Formatted: Font:Not Italic

hsavenije 5/1/2018 08:57  
 Formatted: Font:Not Italic

hsavenije 5/1/2018 09:00  
 Formatted: Font:Italic

135 | The left hand term is the salt flux due to the fresh water of the river that pushes back the salt,  
 136 | whereas the right hand term is the dispersive intrusion of salt due to the exchange flux of the  
 137 | combined mixing processes (see Figure 1). Writing both sides as water fluxes results in:

$$138 \quad Q = \frac{ADS'}{(S-S_f)} \quad (6)$$

139 | The right hand side is the water exchange flux, which is the flux that depletes the gradient. As eq.  
 140 | (6) shows, in steady state this exchange flux is equal to the fresh water discharge. Combination of  
 141 | the flux and the gradient leads to the power of the mixing system per unit length (defined as a  
 142 | positive quantity):

$$143 \quad P = -\rho g Q \frac{\partial z}{\partial x} = \alpha_1 Q \frac{gh}{2} S' \quad (7)$$

144 | Applying the theory of maximum power to the dispersive process, we need to maximize the power  
 145 | with regard to the dispersion coefficient, which is the parameter representing the mixing and which  
 146 | is the main unknown in salt intrusion prediction:

$$147 \quad \frac{dP}{dD} = 0 \quad (8)$$

148 | Applying eq. (8) with constant river discharge  $Q$  and constant depth  $h$  -- the property of an ideal  
 149 | alluvial estuary, according to Savenije (2005) -- leads to:

$$150 \quad \frac{dS'}{dD} = 0 \quad (9)$$

151 | Using the salt balance equation, where  $S' = Q(S - S_f)/(AD)$ , differentiation leads to:

$$152 \quad \frac{dS'}{dD} = \frac{dS'}{dx} \frac{dx}{dD} = \frac{Q}{AD} \left\{ \frac{S'}{D'} - \frac{A'(S - S_f)}{AD'} - \frac{(S - S_f)}{D} \right\} \quad (10)$$

153 | where the prime means the gradient of the parameters with respect to  $x$ . Application of eq. (9) then  
 154 | yields:

$$155 \quad \frac{DS'}{(S - S_f)D'} = \frac{A'D}{AD'} + 1 \quad (11)$$

156 | We introduce three length scales:  $a = -(A - A_f)/A'$ ,  $s = -(S - S_f)/S'$  and  $d = -D/D'$ , where  $a$  is  
 157 | the convergence length of an exponentially varying estuary cross section which tends towards the  
 158 | cross section of the river  $A_f$ ,  $s$  is length scale of the longitudinal salinity variation, and  $d$  is length  
 159 | scale of the longitudinal variation of dispersion. In macro-tidal estuaries, the part of the estuary  
 160 | where the salt intrusion occurs has a much larger cross section than the upstream river, such that  
 161 |  $A_f \ll A$  and  $a \approx -A/A'$ . In riverine estuaries, where this is not the case, a factor  $\epsilon = (1 - A_f/A)$  should be  
 162 | included. All length scales have the dimension of [L]. In an exponentially shaped estuary, the  
 163 | convergence length  $a$  is a constant, but  $d$  and  $s$  vary with  $x$ . It can be shown that the proportion  $s/d$   
 164 | equals the Van der Burgh coefficient  $K (= AD'/Q)$  (Van der Burgh, 1972), which in this approach  
 165 | varies as a function of  $x$ , although generally assumed constant (e.g., Savenije, 2005; Zhang and  
 166 | Savenije, 2017). Using these length scales, eq. (11) can be written as:

$$167 \quad \frac{s}{d} = \frac{a}{a + d\epsilon} \quad (12)$$

168 | or:

$$169 \quad s = \frac{ad}{a + d\epsilon} \quad (12a)$$

170 | or:

hsavenije 5/1/2018 09:05  
 Deleted: To apply

Zhilin Zhang 7/12/2017 13:49  
 Deleted:  $\frac{\partial P}{\partial D} = 0$

Unknown  
 Field Code Changed

Zhilin Zhang 7/12/2017 13:49  
 Deleted:  $\frac{\partial S'}{\partial D} = 0$

Unknown  
 Field Code Changed

Zhilin Zhang 7/12/2017 14:04  
 Deleted:  $\frac{S'}{(S - S_f)} \left\{ \frac{S'}{D'} - \frac{A'(S - S_f)}{AD'} \right\}$

Unknown  
 Field Code Changed

Zhilin Zhang 7/12/2017 14:31  
 Deleted: and

176  $d = \frac{as}{a - s\varepsilon}$  (12b)

177 | where in estuaries with a pronounced funnel shape  $\varepsilon \approx 1$ . Equation (12) is an additional equation to  
 178 | the salt balance, which in terms of the length scales reads:  $s = -AD/Q$ . As a result, we have two  
 179 | differential equations with two unknowns:  $S(x)$  and  $D(x)$ . Adding two boundary conditions at a  
 180 | given point:  $S_0$  and  $D_0$  would solve the system. The first boundary condition is simply the sea  
 181 | salinity if the boundary is chosen at the estuary mouth. Then the only unknown parameter left is the  
 182 | value for the dispersion at the boundary. For this boundary value empirical predictive equations  
 183 | have been developed which relate the  $D_0$  to the estuarine Richardson number (e.g., by Gisen et al.,  
 184 | 2015), which goes beyond this paper. If observations of salinity distributions are available, then the  
 185 | value of  $D_0$  is obtained by calibration.

186 |  
 187 | What the maximum power equation has contributed is that it provides an additional equation. In the  
 188 | past, a solution could only be found if an empirical equation was added describing  $D(x)$ , containing  
 189 | an additional calibration parameter. In the approach by Savenije (2005) this was the empirical Van  
 190 | der Burgh equation containing the constant Van der Burgh coefficient  $K$ . However, with the new  
 191 | equation (12), which in fact represents a spatially varying Van der Burgh coefficient, this additional  
 192 | calibration parameter is no longer required. So this thermodynamic approach replaces the empirical  
 193 | equation by a new physically based equation and removes a calibration parameter, leaving only one  
 194 | unknown: the dispersion at a well-chosen boundary condition.

195 |  
 196 | **3. Application**

197 | The two equations (2) and (12) together can be solved numerically by a simple linear integration  
 198 | scheme. As boundary condition it requires values for  $S_0$  and  $D_0$  at a well-chosen location. In alluvial  
 199 | estuaries the cross-sectional area  $A(x)$  generally varies according to an exponential function which  
 200 | often has an inflection point (see for example Figure 2 describing the Maputo Estuary in  
 201 | Mozambique). The boundary condition is best taken at this inflection point ( $x=x_f$ ) if the estuary has  
 202 | one. If the estuary has no inflection point, as is the case in the Limpopo estuary (see Figure 3), then  
 203 | the boundary condition is taken at the estuary mouth ( $x=0$ ).

204 |  
 205 | The downstream part of estuaries with an inflection point has a much shorter convergence length,  
 206 | giving the estuary a typical trumped shape. This wider part is generally not longer than about 10  
 207 | km, which is the distance over which ocean waves dissipate their energy. Beyond the inflection  
 208 | point, the shape is determined by the combination of kinetic energy of the tide and the potential  
 209 | energy of the river flow. If the tidal energy is dominant over the potential energy of the river, then  
 210 | the convergence is short, leading to a pronounced funnel shape; if the potential energy of the river is  
 211 | large due to regular and substantial flood flows, then the convergence is large, typical for deltas.  
 212 | Hence, the topography can be described by two branches:

213 |  $A = A_f + (A_0 - A_f) \exp(-x/a_0)$  if  $0 < x < x_1$   
 214 |  $A = A_f + (A_1 - A_f) \exp(-(x - x_1)/a_1)$  if  $x \geq x_1$  (13)

215 | where  $A_0$  and  $A_1$  are the cross-sectional areas at  $x=0$  and  $x=x_1$ , respectively, and  $a_0$  and  $a_1$  are the  
 216 | convergence lengths of the lower and upper segments. In some cases, where ocean waves don't  
 217 | penetrate the estuary, there is no inflection point and  $x_1=0$ . The Maputo (see Figure 2) has two  
 218 | segments, whereas the Limpopo Estuary (see Figure 3), an estuary in Mozambique 200 km north of  
 219 | the Maputo, is semi-closed by a sand bar and has a single branch. It can also be seen that in the  
 220 | Limpopo the size of the river cross-section is not negligible and that  $\varepsilon < 1$  showing a slight curve in  
 221 | the exponential functions.

Zhilin Zhang 8/1/2018 16:06  
 Deleted: .

hsavenije 5/1/2018 09:15  
 Deleted: new

Zhilin Zhang 7/12/2017 14:35  
 Deleted: and

hsavenije 5/1/2018 09:15  
 Deleted: for

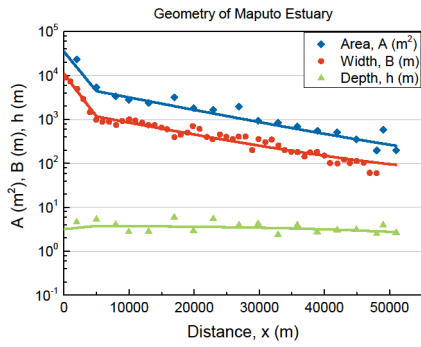
hsavenije 5/1/2018 09:18  
 Deleted: reduces the number of

hsavenije 5/1/2018 09:18  
 Deleted: s

hsavenije 5/1/2018 09:17  
 Deleted: to one: the

229 Subsequently we have integrated the equations (2) and (12) conjunctively by a simple explicit  
230 numerical scheme in a spreadsheet and confronted the solution with observations. The solutions are  
231 fitted to the data by selecting values for  $S$  and  $D$  at the boundary condition  $x=x_1$  (or at  $x=0$  for the  
232 Limpopo). Figures 4 and 5 show applications of the solution to selected observations in the Maputo  
233 and Limpopo estuaries. In the supplementary material more applications are shown, also for other  
234 estuaries in different parts of the world.

235  
236



237

238

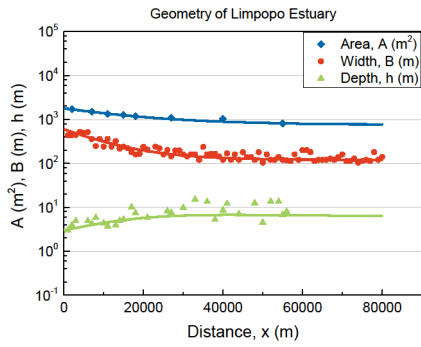
239

240

Figure 2. Geometry of the Maputo Estuary, showing the cross-sectional area  $A$  (blue diamonds), the width  $B$  (red dots) and the depth  $h$  (green triangles) on a logarithmic scale, as a function of the distance from the mouth. The inflection point at  $x_i=5000$  m separates the lower segment with a convergence length of  $a_0=2300$  m from the upper segment with  $a_1=16000$  m.

241

242



243

244

245

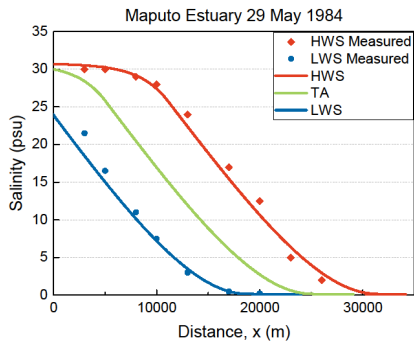
246

Figure 3. Geometry of the Limpopo Estuary, showing the cross-sectional area  $A$  (blue diamonds), the width  $B$  (red dots) and the depth  $h$  (green triangles) on a logarithmic scale, as a function of the distance from the mouth. There is no inflection point, but the estuary converges exponentially towards the river cross section  $A_f=800$  m<sup>2</sup>, with a convergence length of 20 km.

Unknown  
Field Code Changed

Unknown  
Field Code Changed

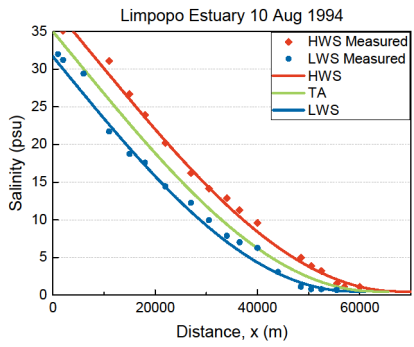




247

248  
249  
250

Figure 4. Application of the numerical solution to observations in the Maputo Estuary for high water slack (HWS) and low water slack (LWS). The green line shows the tidal average (TA) condition. The red diamonds reflect the observations at HWS and the blue dots the observations at LWS on 29 May 1984.



251

252  
253  
254

Figure 5. Application of the numerical solution to observations in the Limpopo Estuary for high water slack (HWS) and low water slack (LWS). The green line shows the tidal average (TA) condition. The red diamonds reflect the observations at HWS and the blue dots the observations at LWS on 10 August 1994.

255  
256

Unknown  
Field Code Changed

Unknown  
Field Code Changed

257 **4. Discussion and conclusion**

258 Making use of the Maximum Power (MP) concept, it was possible to derive an additional equation  
 259 to describe the mixing of salt and fresh water in estuaries. Together with the salt balance equation  
 260 these two first order and linear differential equations only require two boundary conditions (the  
 261 salinity and the dispersion at some well-chosen boundary) to be solved. If the estuary has an  
 262 inflection point in the geometry, then the preferred boundary condition lies there, otherwise the  
 263 boundary condition is chosen at the ocean boundary.

264 This new equation can replace previous empirical equations, such as the Van der Burgh  
 265 equation, and does not require any calibration coefficients (besides the boundary conditions). The  
 266 new equation appears to fit very well to observations, which adds credibility to the correctness of  
 267 applying the MP concept to fresh and salt water mixing.

268 The method presented here is based on a system's perspective, which is holistic rather than  
 269 reductionist. Reductionist theoretical methods have tried to break down the total dispersion in a  
 270 myriad of smaller mixing processes, some of which are difficult to identify or to connect to  
 271 conditions that make them more or less prominent. The idea here is that in a freely adjustable  
 272 system, such as an alluvial estuary, individual mixing processes are not independent of each other,  
 273 but rather influence each other and jointly work at reducing the salinity gradient at maximum  
 274 dissipation. The resulting level of maximum power and dissipation is set by the boundary  
 275 conditions of the system. It then is less important which mechanism is dominant, as long as the  
 276 combined performance is correct. The maximum power limit is a way to derive this joint  
 277 performance of mixing processes. The fact that the relationship derived from maximum power  
 278 works so well in a wide range of estuaries, is an indication that natural systems evolve towards  
 279 maximum power, much like a machine that approaches the maximum performance of the Carnot  
 280 limit.

281 [Appendix A: Notation](#)

282

283

Symbol	Meaning	Dimension	Symbol	Meaning	Dimension
$a$	<a href="#">cross-sectional convergence length</a>	(L)	$Q$	<a href="#">fresh water discharge</a>	(L <sup>3</sup> T <sup>-1</sup> )
$A$	<a href="#">cross-sectional area</a>	(L <sup>2</sup> )	$s$	<a href="#">length scale of the salinity variation</a>	(L)
$A_f$	<a href="#">cross-sectional area of the river</a>	(L <sup>2</sup> )	$S$	<a href="#">salinity</a>	(ML <sup>-3</sup> )
$A_s$	<a href="#">storage cross-sectional area</a>	(L <sup>2</sup> )	$S_f$	<a href="#">freshwater salinity</a>	(ML <sup>-3</sup> )
$B$	<a href="#">width</a>	(L)	$t$	<a href="#">time</a>	(T)
$d$	<a href="#">length scale of the dispersion variation</a>	(L)	$x$	<a href="#">distance</a>	(L)
$D$	<a href="#">dispersion coefficient</a>	(L <sup>2</sup> T <sup>-1</sup> )	$z$	<a href="#">water level</a>	(L)
$g$	<a href="#">gravity acceleration</a>	(LT <sup>-2</sup> )	$\alpha_1$	<a href="#">constant</a>	(-)
$h$	<a href="#">water depth</a>	(L)	$\epsilon$	<a href="#">factor</a>	(-)
$K$	<a href="#">Van der Burgh's coefficient</a>	(-)	$\rho$	<a href="#">density of water</a>	(ML <sup>-3</sup> )
$P$	<a href="#">power per unit length</a>	(MLT <sup>-3</sup> )	$\rho_s$	<a href="#">density of sea water</a>	(ML <sup>-3</sup> )

284

285 | Acknowledgements:  
286 | The authors would like to thank the two reviewers for their valuable comments and two colleagues  
287 | Xin Tian and Sha Lu for specifying the mathematic concepts. The first author is financially  
288 | supported for her PhD research by the China Scholarship Council.

289  
290 | **References:**

- 291  
292 | Fischer, H. B., List, E. J., Koh, R. C. Y., Imberger, J. and Brooks, N. H. (1979) Mixing in Inland  
293 | and Coastal Waters, Academic Press.  
294  
295 | Gisen, J. I. A., Savenije, H. H. G., and Nijzink, R. C. (2015) Revised predictive equations for salt  
296 | intrusion modelling in estuaries, *Hydrology and Earth System Sciences*, 19, 2791-2803.  
297  
298 | Kleidon, A. (2016). Thermodynamic foundations of the Earth system, Cambridge University Press.  
299  
300 | MacCready, P. (2004). Toward a unified theory of tidally-averaged estuarine salinity structure.  
301 | *Estuaries*, 27(4), 561-570.  
302  
303 | Nguyen, A. D., Savenije, H. H. G., van der Wegen, M., and Roelvink, D. (2008) New analytical  
304 | equation for dispersion in estuaries with a distinct ebb-flood channel system. *Estuarine, coastal and*  
305 | *shelf science*, 79(1), 7-16.  
306  
307 | Park, J. K. and James, A. (1990) Mass flux estimation and mass transport mechanism in estuaries.  
308 | *Limnology and Oceanography*, 35(6), 1301-1313.  
309  
310 | Savenije, H. H. G. (2005) Salinity and tides in alluvial estuaries, Elsevier.  
311  
312 | Van der Burgh, P. (1972) Ontwikkeling van een methode voor het voorspellen van zoutverdelingen  
313 | in estuaria, kanalen en zeeën, Rijkswaterstaat Rapport, 10-72.  
314  
315 | Zhang, Z. and Savenije, H.H.G. (2017) The physics behind Van der Burgh's empirical equation,  
316 | providing a new predictive equation for salinity intrusion in estuaries, *Hydrology and Earth System*  
317 | *Sciences*, 21, 3287-3305.  
318  
319  
320

Zhilin Zhang 5/1/2018 10:20

Formatted: English (US)